

RSC Advances



This is an *Accepted Manuscript*, which has been through the Royal Society of Chemistry peer review process and has been accepted for publication.

Accepted Manuscripts are published online shortly after acceptance, before technical editing, formatting and proof reading. Using this free service, authors can make their results available to the community, in citable form, before we publish the edited article. This *Accepted Manuscript* will be replaced by the edited, formatted and paginated article as soon as this is available.

You can find more information about *Accepted Manuscripts* in the [Information for Authors](#).

Please note that technical editing may introduce minor changes to the text and/or graphics, which may alter content. The journal's standard [Terms & Conditions](#) and the [Ethical guidelines](#) still apply. In no event shall the Royal Society of Chemistry be held responsible for any errors or omissions in this *Accepted Manuscript* or any consequences arising from the use of any information it contains.

ARTICLE

TiO₂ immobilized Zein Microspheres: A Biocompatible Adsorbent for Effective Dye Decolourisation

Cite this: DOI: 10.1039/x0xx00000x

Received 00th January 2012,
Accepted 00th January 2012

DOI: 10.1039/x0xx00000x

www.rsc.org/

S. Babitha and Purna Sai Korrapati*

Abstract

Natural protein polymers and metal oxide nano particles individually possess potential dye binding and photo catalytic dye degradation efficiency respectively. To attain the multifunctional property, we have developed a composite Zein-TiO₂ microsphere, characterized and evaluated its dye adsorption and photocatalytic efficiency. The phase structure, morphology, elemental composition and the porous nature of the microspheres were characterized by using X-ray diffractometer (XRD), Fourier transform - infra red (FTIR) spectrophotometer, Field emission - Scanning electron microscope (FE-SEM) with EDAX and Nitrogen adsorption-desorption isotherm measurements. The adsorption experiments performed for different parameters like contact time, initial dye concentration and adsorbent dosage was tested for various adsorption isotherms and kinetics. The results revealed that the Langmuir and Tempkin isotherms were more appropriate and followed pseudo-first order model for the adsorption of acid yellow (AY110) and acid blue (AB113) dyes. The fluorescence probe method was used to confirm the generation of ·OH radicals and elucidated the photodegradation mechanism. Therefore, metallo-polymer based adsorbents provide new scope in the selection of ideal adsorbent for the efficient separation and remediation technology for tannery effluent management.

Introduction

Dyes are widely used in textiles, leather, printing, pulp mills, plastics, and cosmetic industries. Owing to the high fastness and low foaming level properties, acid dyes are comprehensively used in leather dyeing, in spite of its resistance to decomposition, photodegradation and oxidizing agents. Therefore, the discharge of effluent from these industries pose a great threat to the aquatic environment by obstructing light penetration and distress the biological metabolism¹. Due to the mutagenic potential of the aromatic amines of dyes, the metabolites were classified as cytotoxic as well as human carcinogens². Several physical, chemical, biological and electrochemical processes have been employed for the treatment of dye effluent and most of them are incompetent. Toxic by-products and sludge generated from these techniques are difficult to be disposed. To overcome these limitations, unconventional methods were investigated and number of studies has been reported.

Adsorption mode of dye decolourisation is found to be superior among the other treatment methods due to its low cost, pliability in design and ease in operation³. An ideal adsorbent should be biodegradable, inexpensive, and have high affinity to wide range of dyes. Many adsorbents such as activated carbon⁴, clay⁵, chitin⁶, silica⁷, fly ash⁸, zeolites⁹, coir pith¹⁰ and natural polymers¹¹ have been extensively studied for the removal of dyes from aqueous solutions. But still there is a need to find more effective, economical and easily accessible ideal adsorbents. Zein, a by-product of bio ethanol industry is widely used for its biodegradable and biocompatible properties¹². However, only few reports are available for its use as an adsorbent for environmental cleanup. Different types of nano structured materials like titanium dioxide¹³, bi metallics¹⁴, carbon nanotubes¹⁵ and magnetic nanoparticles¹⁶ were investigated for environmental treatments. Metal and metal oxide nanoparticles gained enormous significance owing to its unique properties in regard to sorption behaviours, magnetic activity, chemical reduction, ligand sequestration amongst others¹⁷. The excellent chemical stability, non toxicity and photo-catalytic activities of TiO₂ nanoparticles have attracted more attention towards self-cleaning, anti-bacterial, UV protection. It has also proved to be useful in environmental

Biomaterials Department, CSIR, Central Leather Research Institute, Chennai, India-600 020. E-mail: purnasaik.clri@gmail.com; Tel: +91-44-24437263/+91-44-24453491

applications like organic waste and waste water treatment processes¹⁸. These effects are mainly due to the formation of hydroxyl radicals (OH^\cdot) and superoxide ion radicals (O_2^\cdot) in the presence of light¹⁹. Further by surface modification²⁰ or conjugating with a charge transfer catalyst, doping with metal and non metal ions, blending with polymers, metal oxides and coupling with semiconductors precludes aggregation and results in uniform distribution and enhanced photo response and photocatalytic dye degradation efficiency²¹. Therefore attempts are being continuously made to develop a hybrid nano composite with improved durability, robust mechanical strength, and excellent sorption characteristics for multitude of applications²²⁻²⁴. The hybrid nanocomposites such as Ag and Ti doped BiOI ²⁵, Chitosan-ZnO²⁶⁻²⁷, Magnetic Chitosan composite²⁸, AgNPs coated activated carbon²⁹, Polyaniline/Iron Oxide composite³⁰, ZnO polymeric hybrid beads³¹ have been reported for dye adsorption. The combination of Zein and TiO_2 , which individually possess excellent dye adsorption and degradation property, would prove as an efficient alternative as a composite material for environmental cleanup.

In this study, we have attempted to tailor the Zein- TiO_2 microspheres as an adsorbent with high adsorption and photocatalytic dye degradation capacity, which combines the advantages of inorganic metal oxides (large surface area, inertness, cheapness) and natural polymers (thermal stability, biodegradability). The effects of initial dye concentration, contact time, adsorbent dosage, dye removal efficiency, adsorption equilibrium, isotherm and kinetics of dye adsorption and the photo degradation mechanism reveal an ideal metallo-polymer composite for removing the toxic dyes from tannery effluents.

Results and discussion

Physico-chemical characterization of adsorbent

The X-ray diffraction analysis revealed the nature of the synthesized microspheres. The broad peak at 19.44° corresponds to the native zein structure³² and the diffraction angles at 25.15° , 37.38° , 47.99° , and 62.92° matching the planes 101, 004, 200, 204 confirmed the presence of anatase phase of TiO_2 nanoparticles in zein microspheres (Fig.1).

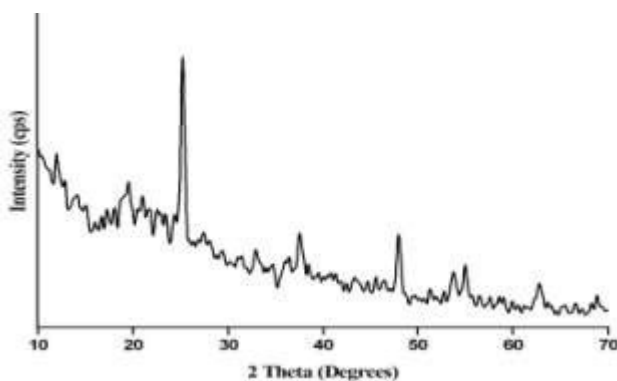


Fig.1 X-ray diffraction pattern of Zein- TiO_2 microspheres

The immobilization of TiO_2 nanoparticles on Zein microspheres were confirmed by the FTIR analysis. The FTIR

spectrum of only zein microspheres (Fig.2a) showed characteristic peaks at $1,658\text{ cm}^{-1}$, $1,537\text{ cm}^{-1}$, and $1,238\text{ cm}^{-1}$ corresponding to amide I, II, and III, respectively. The contribution of TiO_2 dominated the spectrum of Zein - TiO_2 microspheres (Fig. 2b). The decrease of the band related to primary amine groups at $1450\text{--}1650\text{ cm}^{-1}$; $3300\text{--}3500\text{ cm}^{-1}$; and $700\text{--}800\text{ cm}^{-1}$ revealed the immobilization of TiO_2 on the surface of zein microspheres. The peak located at 1088 cm^{-1} assigned to C-O stretching shifted to lower wavelength of 1038 cm^{-1} . The surface modification of TiO_2 nanoparticles by APTMS, showed asymmetrical and symmetrical stretching vibrations of the C-H bond in methylene group at 2928 and 2870 cm^{-1} . Furthermore, the peak corresponding to Si-O-Si bond was observed at around 1040 cm^{-1} indicating the condensation reaction between silanol groups. The peak of Si-O-Si bond was much stronger, and the N-H bending vibration of primary amines (NH_2) was observed as a broad band in the region $1605\text{--}1560\text{ cm}^{-1}$. The appearance of these bands demonstrated that amine functional groups in organosilane were grafted onto the modified particle surface.

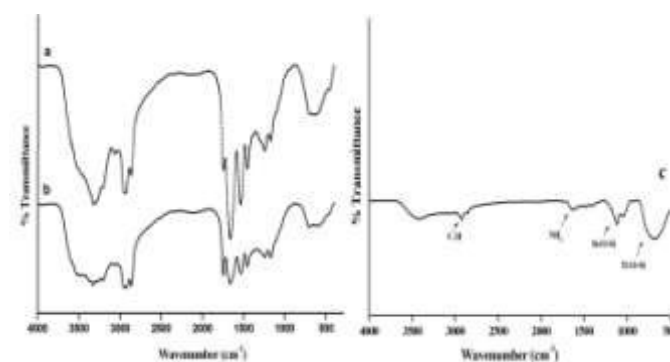


Fig.2 FT-IR spectra of (a) Zein microspheres (b) Zein- TiO_2 microspheres and (c) silanized TiO_2 nanoparticles.

The surface morphology and the elemental characterization at a specific position of the Zein - TiO_2 microspheres was evident from the FE-SEM and EDAX image. The irregular and porous structure of the microspheres as indicated by arrows can attribute for effective dye adsorption (Fig.3a and 3b).

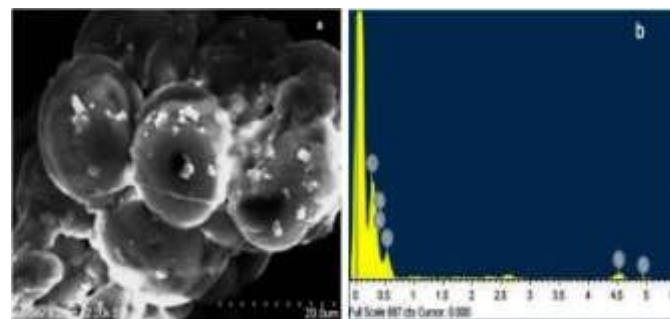


Fig.3 Field Emission - Scanning Electron Micrograph of Zein - TiO_2 Microspheres (a) EDAX analysis (b).

The nitrogen adsorption-desorption isotherm of the Zein-TiO₂ microspheres shown in Fig.4 belongs to type IV profile according to the IUPAC classification with a pronounced hysteresis for partial pressure $P/P_0 > 0.45$. It is an indicative of the presence of mesoporous structure and multilayer adsorption on the outer surface of the particles³³. The specific surface area of the prepared Zein-TiO₂ microspheres is $37.37 \pm 0.457 \text{ m}^2/\text{g}$ which was calculated using BET method. According to the desorption isotherm, the average pore volume and pore diameter is $0.132 \text{ cm}^3/\text{g}$ and 22 nm based on the BJH model.

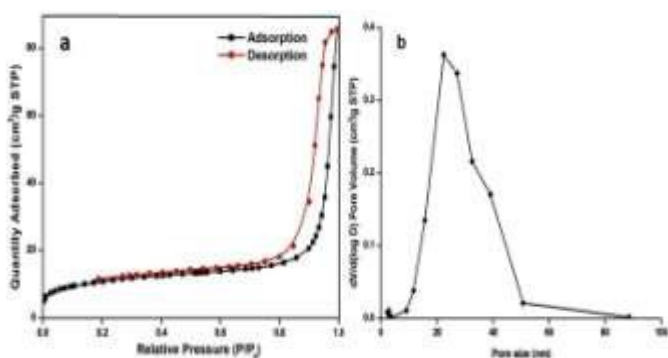


Fig.4 Nitrogen adsorption-desorption isotherm (a), and Pore size distribution curve of Zein – TiO₂ microspheres (b).

Effect of contact time

The UV-Vis spectra showed the effect of microspheres on dye degradation in terms of absorbance data over a wavelength range of two different dyes. The characteristic absorption peak of AY110 and AB113 were at 420 and 565nm, respectively. The greater the intensity of the peak, the lower the adsorption rate of dye to the adsorbent. The increased degradation rate resulted in lower absorbance reading. The peak became gradually smoother with increased contact time, signifying that the adsorption and sufficient photocatalytic reaction has been gained to remove the maximum dye from the solution which was clearly evident from (Fig.5a & b).

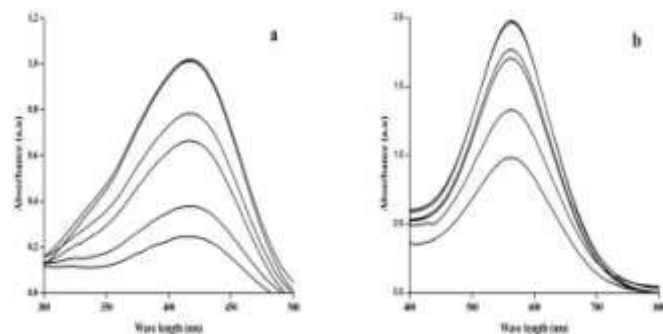


Fig.5 Effect of contact time on the removal of (a) AY110 and (b) AB113 by Zein-TiO₂ microspheres.

The loading of TiO₂ nanoparticle on zein microspheres serves as an important factor for dye removal by affecting the number

of active sites on the surface and leads to OH⁻ generation when exposed to light. Under UV or Visible light irradiation, the TiO₂ incorporated zein microspheres generate hydroxyl radicals on the surface which initiates various oxidation reactions, thereby enhanced the degradation rate of dye pollutants. This has been elucidated in (Fig.6) using fluorescence probe method. Hence increase in TiO₂ loading resulted in excellent photo catalytic activity and enhanced dye degradation rate.

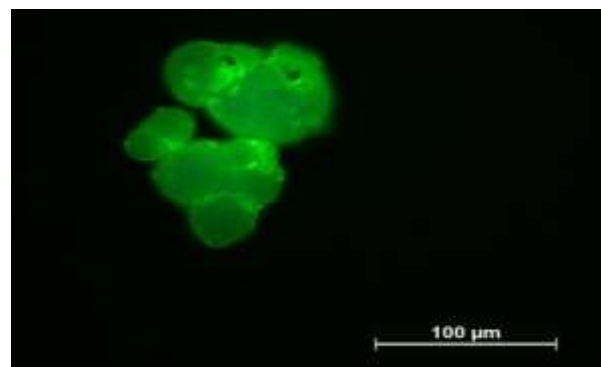


Fig.6 Fluorescence analysis of reactive oxygen species (Hydroxyl radicals) generation on the surface of Zein – TiO₂ microspheres.

Effect of initial dye concentration

The effect of initial dye concentration and the percentage of dye removal were shown in (Fig.7a & b). The adsorption efficiency of AY110 and AB113 were evaluated by determining the percentage decrease of the absorbance at 420 and 565nm respectively. It is apparent that higher the initial dye concentration, lower the percentage of dye adsorbed. The percentage dye removal efficiency reached up to a maximum of 96% and 89% at lower concentration (10mg/L) and decreased to 77% and 61% at a higher concentration (100mg/L) of AY110& AB113 respectively. Owing to the availability of free binding sites on the adsorbent, the low initial dye concentration leads to higher dye removal efficiency and a high concentration resulted in low adsorption efficiency due to its already occupied binding sites.

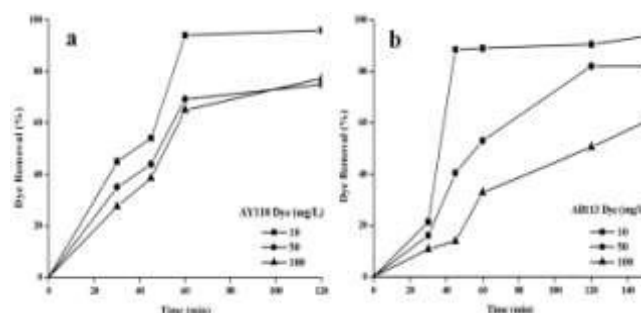


Fig.7 Effect of initial dye concentration on dye removal (a) AY110 and (b) AB113 by Zein – TiO₂ microspheres.

Effect of adsorbent dosage

The effect of Zein- TiO₂ microsphere dosage on dye removal was studied by adding dye solution with an initial concentration of 100mg/L at room temperature with constant stirring speed of 100rpm. Different amounts of Zein - TiO₂ microspheres (0.5, 1, and 1.5, 2g/l) were added to test the dye removal competence. After equilibrium, the solution samples were centrifuged and the concentration of dye in the supernatant was analyzed. The plot of dye removal (%) Vs adsorbent dosage (g/L) was represented (Fig.8).

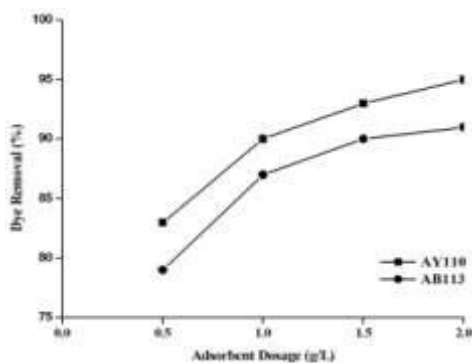


Fig.8 Effect of adsorbent (Zein-TiO₂ microspheres) dosage on the adsorption of dyes.

Adsorption isotherms

The interaction behaviour of adsorbate and the adsorbent can be expressed by several adsorption isotherm models. The data were analyzed by the following equilibrium adsorption isotherms namely, Langmuir, Freundlich and Tempkin isotherm. The Langmuir isotherm has been successfully applied to a number of sorption methods to explain the adsorption mechanism. The basic assumption is that sorption takes place at specific sites on the surface of adsorbent where the adsorbate is strongly attracted³⁴. This can be expressed as follows:

$$\frac{C_e}{Q_e} = \frac{1}{K_L Q_0} + \frac{C_e}{Q_0}$$

Where,

C_e - the equilibrium concentration of dye solution (mg/L),

Q_e - the amount of dye adsorbed on Zein-TiO₂ microspheres at equilibrium (mg/g),

K_L - Langmuir constant (L/g) and

Q_0 - the maximum adsorption capacity (mg/g).

The essential characteristic term of Langmuir equation can be expressed by R_L , the dimensionless separation factor which is represented as,

$$R_L = \frac{1}{1 + K_L C_0}$$

Where,

C_0 - the initial dye concentration (mg/L),

R_L - indicates the type of isotherm whether it is favourable ($0 < R_L < 1$), unfavourable ($R_L > 1$), linear ($R_L = 1$) or irreversible ($R_L = 0$).

On the other hand, Freundlich isotherm takes into account heterogeneous system which is not restricted to monolayer adsorption³⁵. This can be expressed as:

$$\ln q_e = \ln K_F + \frac{1}{n} \ln C_e$$

Where,

K_F - the adsorption capacity at unit concentration (mg/L)

$1/n$ - adsorption intensity.

The value of $1/n$ indicates the nature of isotherm. If $1/n < 0$ then the isotherm is irreversible, and more heterogeneous if $1/n = 0$, or has a favourable surface heterogeneity (if $0 < 1/n < 1$) or a cooperative adsorption if $1/n > 1$.

Tempkin model assumes that the rate of adsorption in the layer decreases linearly with coverage due to adsorbent - adsorbate interactions and it is characterized by uniform distribution of binding energies, up to a maximum binding energy³⁶. The isotherm is given as follows:

$$q_e = B_1 \ln K_T + B_1 \ln C_e$$

Where,

K_T - the equilibrium binding constant (L/mol) corresponding to the maximum binding energy and B_1 - a constant related to the heat of adsorption.

The correlation coefficients of Langmuir, Freundlich and Tempkin isotherms are given in (Table. 1). The correlation coefficient implies that Langmuir and Tempkin isotherms are more appropriate for adsorption of AY110 and AB113 on Zein - TiO₂ microspheres. Moreover, the dimensionless constant R_L (0.14 & 0.193) revealed that the adsorption is favourable and irreversible and K_T (234 & 295) showed the maximum binding energy.

Table.1: Linearised isotherm coefficients

Langmuir isotherm				Freundlich isotherm			Tempkin isotherm		
Q_0	K_L	R_L	r^2	K_F	n	r^2	K_T	B_1	r^2
AY110									
25	0.057	0.14	0.9948	7.1343	1.15	0.94	234	48.78	0.96
AB113									
12.84	0.041	0.193	0.9908	12.58	0.44	0.97	295	63.45	0.99

Adsorption kinetics

The mechanism of solute sorption onto a sorbent can be expressed by several adsorption kinetic models. The characteristic constants have to be determined in order to predict the rate at which a solute is removed from the aqueous solution using pseudo - first order³⁷ and pseudo- second order³⁸ kinetic models by the following equations:

$$\ln (Q_e - Q_t) = \ln Q_e - k_1 t$$

$$\frac{t}{Q_t} = \frac{1}{k_2 Q_e^2} + \left(\frac{1}{Q_e} \right) t$$

Where,

Q_e , Q_t - the amount of dye adsorbed at equilibrium (mg/g), at time t (mg/g) respectively

k_1 , k_2 - equilibrium rate constants of pseudo-first order kinetics (1/min) and pseudo-second order kinetics ($\text{g mg}^{-1}\text{min}^{-1}$) respectively.

The adsorption kinetic plots are shown in (Fig.9 & 10) and the kinetic parameters are listed in (Table. 2). The calculated correlation coefficients are closer to unity for pseudo - first order kinetic model than the second order kinetics (0.99 Vs 0.94) and therefore the rate of sorption follows pseudo - first order with good correlation.

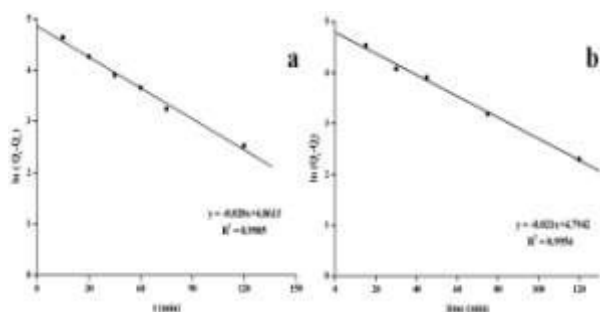


Fig.9 Pseudo-first order kinetic model for adsorption of (a) AY110 & (b) AB113 on Zein - TiO_2 microspheres.

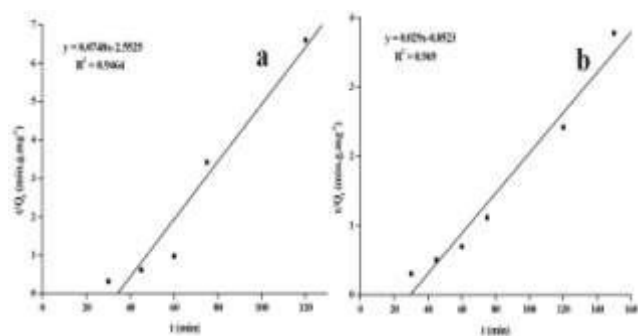


Fig.10 Pseudo-second order kinetic model for adsorption of (a) AY110 & (b) AB113 on Zein - TiO_2 microspheres.

Table.2: Kinetics constants for pseudo-first and pseudo-second order model

	Pseudo - first order			Pseudo - second order		
	Q_e	K_1 (min^{-1})	R^2	Q_e	K_2 ($\text{g mg}^{-1}\text{min}^{-1}$)	R^2
AY110	129.19	0.020	0.9905	13.36	0.0021	0.9464
AB113	128.8	0.02	0.9954	34.48	0.0009	0.9690

Intra particle diffusion

Intra particle diffusion model is to determine the common functional relationship to adsorption process, where uptake varies almost proportionally with $t^{1/2}$ rather than with contact time t .

$$q_t = K_{id} t^{1/2} + C$$

Where K_{id} is the intraparticle diffusion rate constant and C is the intercept. The intercept gives an idea about the thickness of the boundary layer i.e. the larger the intercept, the greater the boundary layer effect³⁹. It also indicates that there is some degree of boundary layer control as it does not pass through the origin⁴⁰. The diffusion rate constants are shown in (Table. 3). The value of intra particle diffusion rate constant clearly showed that the boundary layer has significant effect on the diffusion mechanism of dye uptake by Zein - TiO_2 microspheres.

Table.3: Intra particle Diffusion rate constants

	Intra particle diffusion		
	K_{id}	C	r^2
AY110	9.78	41.36	0.9828
AB113	7.25	28.54	0.9763

Experimental

Materials

Zein, 3-Amino propyl tri methoxy silane (APTMS), Dimethyl sulfoxide (DMSO) from Sigma-Aldrich. TiO_2 nanoparticles, Sesame oil, Span 80, Petroleum ether were used without any pre-treatment. The leather dyes, Acid Yellow (AY110) and Acid Blue (AB113) were obtained from the tannery department of CLRI and used as a model pollutant.

Surface modification of TiO_2 nanoparticles

The titanium dioxide nanoparticles were synthesised using microbial methods as described by Babitha et al⁴¹. The agglomeration of nanoparticles can be prevented by the surface functionalisation of TiO_2 nanoparticles which would further enhance the durability, dispersion and compatibility of the nanoparticles. The surface modification was carried out by a silane coupling agent, 3-aminopropyltrimethoxysilane (APTMS) without disturbing the inherent properties of the nanoparticles⁴². The synthesised TiO_2 nanoparticles were dispersed in 50 ml dimethyl sulfoxide (DMSO) and ultra sonicated for 1 hour. Then, silane coupling agent (APTMS) was added in the dispersion and kept refluxing for about 3 hours. The dispersed particles were separated out from solvent by centrifugation (10 min at 10,000 rpm). The excess silanes were removed by washing thrice with ethanol and water,

alternatively. The pellet was re-dispersed in a fresh solvent and sonicated for about 10 minutes to ensure uniform dispersion before centrifugation. The modified particles were dried in an oven at 60°C overnight and cooled in a vacuum chamber for 1 h at room temperature.

Preparation of zein - TiO₂ microspheres

The microspheres were prepared in accordance to the method of Karthikeyan et al⁴³. Solution blending is carried out to attain a molecular level of mixing. Directly, the silanized nanoparticles and polymer was mixed in solvent (90% Ethanol) and kept under stirring for about 30 min. The solution was added to the continuous phase (sesame oil) containing 0.5% span 80 as an emulsifying agent. The mixture was then agitated using a homogenizer with a rotating speed of 500 rpm. The dispersed TiO₂ nanoparticles and zein solution was immediately transformed into fine droplets, which was subsequently solidified into rigid microspheres due to solvent evaporation. The particles were finally collected by filtration, washed extensively with petroleum ether, and desiccated under vacuum for 24 hours.

Physico-chemical characterization of adsorbent

The powder X-ray diffraction (XRD) patterns were evaluated using X-ray diffractometer with CuK α radiation ($\lambda = 1.5405\text{\AA}$) over a wide range of Bragg angles ($10^\circ \leq 2\theta \leq 70^\circ$). The scanning was done at 0.02°/min with the time constant of 2s.

Fourier transformed infrared (Perkin Elmer – Spectrum One) spectra of silanized TiO₂ nanoparticles, Zein-TiO₂ microspheres were obtained by mixing samples with potassium bromide, compressed into a pellet by applying 1 ton/unit. Spectral scanning was done in the range of 4,000–400 cm⁻¹.

The surface morphology of the Zein - TiO₂ microsphere was examined by scanning electron microscope (SEM, Hitachi SU-6600). The microspheres were vacuum dried, mounted onto brass stub, and sputter coated with gold in argon atmosphere and operated at a voltage of 15 kV. The elemental composition of the microsphere at a specific position was analyzed using energy dispersive X-ray spectroscopy.

The nitrogen adsorption-desorption isotherms were measured at -196°C using a Micromeritics ASAP 2020 analyzer. The sample was degassed prior to the characterization. The specific surface area was calculated according to the BET⁴⁴ (Brunauer-Emmett and Teller) model, whereas the pore size and average pore volume were calculated using the BJH⁴⁵ (Barrett-Joyner-Halenda) formula based on the desorption data of the isotherms. Fluorescence was employed to detect the reactive oxygen species (mainly ·OH) radical using 2, 7-dichlorodihydrofluorescein (DCFH) as a fluorescence probe molecule⁴⁶. The probe solution was prepared by dispersing 0.5ml of 1mM DCFH-DA ethanol solution in 2ml of 0.01M NaOH aqueous solution and allowed to stand in dark for 30 min to generate DCFH. Then the above mixture was diluted to 5μM with 0.1M PBS buffer to obtain the final probe solution. The Zein-TiO₂ microspheres were dispersed in the above solution to form 50μg/ml suspension. The suspension was then exposed to UV/ visible light irradiation for 20 min. After irradiation, the fluorescence was observed using Leica fluorescence microscope with the excitation wavelength at 488nm⁴⁷.

Adsorption studies

The effects of contact time, initial dye concentration and adsorbent dosage for the removal of acid dyes, AY110 and AB113 from aqueous solutions were evaluated. The dye adsorption measurements were conducted by mixing optimum amount of Zein- TiO₂ microspheres (1mg/ml) in varied concentrations (10, 50 and 100mg/l) of dye solution, with an agitation speed of 100 rpm. The change in the absorbance of all samples were monitored and determined at different time intervals during the adsorption process. At the end of the experiments, the solution samples were centrifuged and the dye concentration was measured using a UV-Visible spectrophotometer at 420nm and 565nm respectively. The amount of adsorbed dye, Q (mg/g), was calculated by

$$Q_e = (C_o - C_e) \frac{V}{W}$$

where,

C_o - initial concentration (mg/L),

C_e - equilibrium concentration (mg/L),

V - volume of dye solution (L) and

W - weight (g) of the adsorbent.

$$\text{Percentage removal} = \frac{(C_i - C_e)}{C_i} \times 100$$

The dye removal efficiencies under different conditions were also calculated from the difference between the initial and equilibrium concentrations of the solution. The results were verified using the adsorption isotherms (Langmuir, Freundlich and Tempkin) and kinetics (pseudo first order, pseudo second order and intraparticle diffusion model).

Conclusions

The biocompatible and biodegradable Zein-TiO₂ microspheres were synthesized, characterized and the dye adsorption properties were investigated. The XRD, FTIR, FE-SEM and EDAX results confirmed the presence of anatase TiO₂ NPs on zein microspheres. The porosity measurements by N₂ adsorption-desorption technique revealed the pore size distribution and the mesoporous nature of the material. Adsorption isotherms and kinetic studies were performed and the results showed that the equilibrium data followed Langmuir and Tempkin isotherms for AY110 and AB113 respectively. The adsorption kinetics followed the Pseudo-first-order model. Being a low-cost and eco friendly adsorbent with the combined advantage of, TiO₂ nanoparticles and agro-industrial by-product Zein, the Zein - TiO₂ microspheres showed maximum adsorption and photocatalytic dye degradation efficiency. The degradation mechanism is also elucidated by the fluorescence

probe method. The promising results showed that it could be used as an effective alternative for the removal of acid dyes from aqueous solutions. The study therefore, opens up new methods for efficient treatment of tannery effluent to reduce the dye toxicity.

Acknowledgements

The authors thank the Director, CSIR – CLRI for his constant support. The authors also thank Dr. NK Chandra Babu, Chief Scientist, Leather Processing Department, CSIR – CLRI for providing the dye samples. The first author gratefully acknowledges the DST – INSPIRE, New Delhi for the fellowship (IF110583).

References

- V. K. Gupta and Suhas, *J. Environ. Manage.*, 2009, **90**, 2313–42.
- N. Mathur, P. Bhatnagar and P. Sharma, *Univers. J. Environ. Res. Technol.*, 2012, **2**, 1–18.
- G. Crini, *Bioresour. Technol.*, 2006, **97**, 1061–1085.
- V. Meshko, L. Markovska, M. Mincheva and a. Rodrigues, *Water Res.*, 2001, **35**, 3357–3366.
- G. Atun, G. Hisarli, W. S. Sheldrick and M. Muhler, *J. Colloid Interface Sci.*, 2003, **261**, 32–39.
- S. a Figueiredo, J. M. Loureiro and R. a Boaventura, *Water Res.*, 2005, **39**, 4142–52.
- Y. Badr, M. G. Abd El-Wahed and M. a Mahmoud, *J. Hazard. Mater.*, 2008, **154**, 245–53.
- P. Janos, H. Buchtová and M. Rýznarová, *Water Res.*, 2003, **37**, 4938–44.
- S. Babel and T. A. Kurniawan, 2003, **97**, 219–243.
- C. Namasivayam and D. Kavitha, *Dye. Pigment.*, 2002, **54**, 47–58.
- G. Z. Kyzas, M. Kostoglou, N. K. Lazaridis and D. N. Bikiaris, in *EcoFriendly Textile Dyeing and Finishing*, 2013, pp. 177–206.
- A. R. Patel and K. P. Velikov, *Curr. Opin. Colloid Interface Sci.*, 2014.
- C. C. Chen, C. S. Lu, Y. C. Chung and J. L. Jan, *J. Hazard. Mater.*, 2007, **141**, 520–8.
- P. Wilhelm and D. Stephan, *J. Photochem. Photobiol. A Chem.*, 2007, **185**, 19–25.
- T. A. Saleh, in *Synthesis and Applications of Carbon Nanotubes and Their Composites*, 2013, pp. 479–493.
- N. M. Mahmoodi, J. Abdi and D. Bastani, *J. Environ. Heal. Sci. Eng.*, 2014, **12**, 96.
- J. Zhang, Z. Xiong and X. S. Zhao, *J. Mater. Chem.*, 2011, **21**, 3634.
- W.-C. Lin, W.-D. Yang and S.-Y. Jheng, *J. Taiwan Inst. Chem. Eng.*, 2012, **43**, 269–274.
- J. Zhang and Y. Nosaka, *J. Phys. Chem. C*, 2014, **118**, 10824–10832.
- B. Gradzik, M. E. L. Fray, E. Wiśniewska and W. Pomeranian, 2011, **2**, 4–6.
- H. Arora, C. Doty, Y. Yuan, J. Boyle, K. Petras and B. Rabatic, *Titanium Dioxide Nanocomposites*, 2010, vol. 8.
- S. Sarkar, E. Guibal, F. Quignard and a. K. SenGupta, *J. Nanoparticle Res.*, 2012, **14**, 715.
- C. Shen, S. Song, L. Zang, X. Kang, Y. Wen, W. Liu and L. Fu, *J. Hazard. Mater.*, 2010, **177**, 560–6.
- G. Zaccariello, E. Moretti, L. Storaro, P. Riello, P. Canton, V. Gombac, T. Montini, E. Rodríguez-Castellón and a. Benedetti, *RSC Adv.*, 2014, **4**, 37826.
- Y. S. Yohan Park, Yulyi Na, Debabrata Pradhan, Bong-Ki Min, *CrystEngComm*, 2014, **16**, 3155–3167.

- 26 R. Salehi, M. Arami, N. M. Mahmoodi, H. Bahrami and S. Khorramfar, *Colloids Surf. B. Biointerfaces*, 2010, **80**, 86–93.
- 27 W. S. Wan Ngah, L. C. Teong and M. a. K. M. Hanafiah, *Carbohydr. Polym.*, 2011, **83**, 1446–1456.
- 28 L. W. Peng Wang, Tingguo Yan, *Bioresources*, 2013, **8**, 6026–6043.
- 29 J. Pal, M. K. Deb, D. K. Deshmukh and D. Verma, *Appl. Water Sci.*, 2013, **3**, 367–374.
- 30 S. A. Jebreil, *Int. J. Chem. Nucl. Metall. Mater. Eng.*, 2014, **8**, 1336–1341.
- 31 H. Shokry Hassan, M. F. Elkady, a. H. El-Shazly and H. S. Bamufleh, *J. Nanomater.*, 2014, **2014**, 1–14.
- 32 H. Lai, P. H. Geil and G. W. Padua, *J. Appl. Polym. Sci.*, 1998, **71**, 1267–1281.
- 33 Y. Zhang, S. Zhang, K. Wang, F. Ding and J. Wu, *J. Nanomater.*, 2013, **2013**.
- 34 I. Langmuir, *J. Am. Chem. Soc.*, 1916, **252**, 2221–2295.
- 35 M. B. Desta, *J. Thermodyn.*, 2013, 1–6.
- 36 Y. Kim, C. Kim, I. Choi, S. Rengaraj and J. Yi, *Environ. Sci. Technol.*, 2004, **38**, 924–931.
- 37 C. Lee, H. Kim, I. Jang, J. Im and N. Park, *Appl. Mater. Interfaces*, 2011, **3**, 1953–1957.
- 38 G. M. Y.S.Ho, *Chem. Eng. J.*, 1998, **70**, 115–124.
- 39 A. Ozcan and a S. Ozcan, *J. Hazard. Mater.*, 2005, **125**, 252–9.
- 40 W. Plazinski and W. Rudzinski, *J. Phys. Chem. C*, 2009, **113**, 12495–12501.
- 41 S. Babitha and P. S. Korrapati, *Mater. Res. Bull.*, 2013, **48**, 4738–4742.
- 42 J. Zhao, M. Milanova, M. M. C. G. Warmoeskerken and V. Dutschk, *Colloids Surfaces A Physicochem. Eng. Asp.*, 2012, **413**, 273–279.
- 43 K. Karthikeyan, R. Lakra, R. Rajaram and P. S. Korrapati, *AAPS PharmSciTech*, 2012, **13**, 143–9.
- 44 S. Brauner, P.H. Emmett, E. Teller, *J. Am. Chem. Soc.*, 1938, **60**, 309–319.
- 45 Elliott P. Barrett, Leslie G. Joyner, Paul P. Halenda, *J. Am. Chem. Soc.*, 1951, **73**, 373–380.
- 46 A. Gomes, E. Fernandes and J. L. F. C. Lima, *J. Biochem. Biophys. Methods*, 2005, **65**, 45–80.
- 47 L. Sun, Y. Qin, Q. Cao, B. Hu, Z. Huang, L. Ye and X. Tang, *Chem. Commun. (Camb.)*, 2011, **47**, 12628–30.